Supernova 1987A:30 years later - Cosmic Rays and Nuclei from Supernovae and their aftermaths
Proceedings IAU Symposium No. 331, 2017
A. Marcowith, M. Renaud, G. Dubner, A. Ray & A. Bykov, eds.

doi:10.1017/S1743921317004434

Detecting Thermal X-Ray Emission and Proper Motions in RX J1713.7-3946

Satoru Katsuda[1], Fabio Acero[2], Nozomu Tominaga[3,4], Jean Ballet[2], Yasuo Fukui[5], Junko S. Hiraga[6], Katsuji Koyama[7], Shiu-Hang Lee[8], Koji Mori[9], Shigehiro Nagataki[10], Yutaka Ohira[11], Robert Petre[12], Hidetoshi Sano[5,13], Yoko Takeuchi[14], Toru Tamagawa[14], Naomi Tsuji[15], Hiroshi Tsunemi[16] and Yasunobu Uchiyama[15]

[1]Department of Physics, Faculty of Science & Engineering, Chuo University, 1-13-27 Kasuga, Bunkyo, Tokyo 112-8551, Japan
email: katsuda@phys.chuo-u.ac.jp

[2]Laboratoire AIM, IRFU/SAp – CEA/DRF – CNRS – Universite Paris Diderot, Bat. 709, CEA-Saclay, Gif-sur-Yvette Cedex, France

[3]Department of Physics, Faculty of Science and Engineering, Konan University, 8-9-1 Okamoto, Kobe, Hyogo 658-8501, Japan

[4]Kavli Institute for the Physics and Mathematics of the Universe (WPI), The University of Tokyo, 5-1-5 Kashiwanoha, Kashiwa, Chiba 277-8583, Japan

[5]Department of Physics, Nagoya University, Furo-cho, Chikusa-ku, Nagoya 464-8601, Japan

[6]Department of Physics, School of Science and Technology, Kwansei Gakuin University, Sanda 669-1337, Japan

[7]Department of Physics, Graduate School of Science, Kyoto University, Kitashirakawa Oiwake-cho, Sakyo-ku, Kyoto 606-8502, Japan

[8]Department of Astronomy, Kyoto University, Kitashirakawa-Oiwake-cho, Sakyo-ku, Kyoto 606-8502, Japan

[9]Department of Applied Physics and Electronic Engineering, Faculty of Engineering, University of Miyazaki, 1-1 Gakuen Kibanadai-Nishi, Miyazaki 889-2192, Japan

[10]Astrophysical Big Bang Laboratory, Riken, Wako, Saitama 351-0198, Japan

[11]Department of Physics and Mathematics, Aoyama-Gakuin University, Sagamihara, Kanagawa 252-5258, Japan

[12]Astrophysics Science Division, NASA Goddard Space Flight Center, Greenbelt, MD 20771, USA

[13]Institute for Advanced Research, Nagoya University, Furo-cho, Chikusa-Ku, Nagoya 464-8601, Japan

[14]High Energy Astrophysics Laboratory, RIKEN Nishina Center, 2-1 Hirosawa, Wako-shi, Saitama 351-0198, Japan

[15]Department of Physics, Rikkyo University, 3-34-1 Nishi-Ikebukuro, Toshima, Tokyo 171-8501, Japan

[16]Department of Earth and Space Science, Osaka University, 1-1 Machikaneyama-cho, Toyonaka, Osaka 560-0043, Japan

Abstract. We report detections of thermal X-ray line emission and proper motions in the supernova remnant (SNR) RX J1713.7-3946, the prototype of the small class of synchrotron dominated SNRs. Based on deep XMM-Newton observations, we find clear line features including Ne Lyα, Mg Heα, and Si Heα from the central portion of the remnant. The metal abundance ratios suggest that the thermal emission originates from core-collapse SN ejecta arising from a relatively low-mass ($\lesssim$20 $M_\odot$) progenitor. In addition, using XMM-Newton observations on a 13 yr time interval, we have measured expansion in the southeastern rim to be $\sim$0.75″ yr^{-1} or

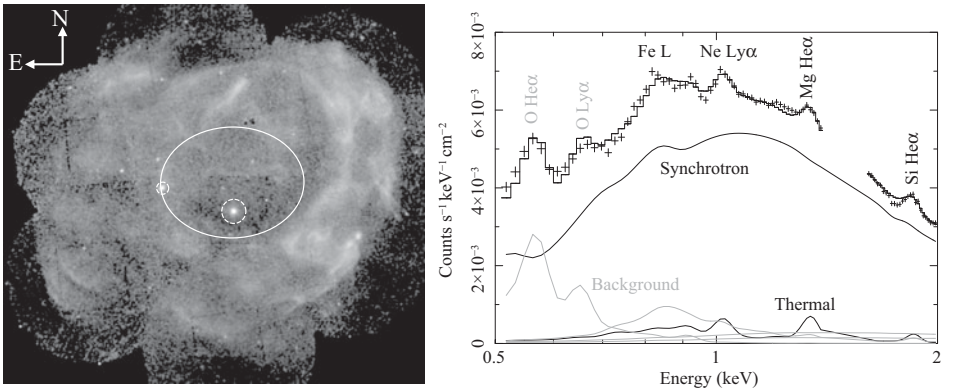

Figure 1. Left: XMM-Newton's surface brightness map of the entire RX J1713.7-3946. The large white ellipse shows where we extract spectrum shown in the right-hand panel. Two small white ellipses show regions where we excluded point-like sources from our spectral analysis. Right: Non X-ray background-subtracted XMM-Newton's MOS1+2 spectrum extracted from the ellipse in the left-hand panel. Solid curves represent the best-fit model. Note that the energy band of 1.4–1.6 keV is ignored owing to the imperfect subtraction of the instrumental Al-K line emission.

$\sim$3500 km s^{-1} at a distance of 1 kpc. Given this, we derive an upstream density to be $\sim$0.01 cm^{-3}, compatible with the lack of thermal X-rays from the shocked ambient medium. We also estimate the age of the remnant to be $\sim$1200–1600 yr, roughly consistent with the idea that RX J1713.7-3946 is the remnant of SN 393.

Keywords. shock waves, ISM: abundances, ISM: individual (RX J1713.7-3946)

1. Introduction

Synchrotron X-ray emission has been ubiquitously detected from shells of young supernova remnants (SNRs), following the first discovery in SN 1006 (Koyama *et al.* 1995). This is clear evidence that electrons are accelerated to very high energies (up to $\sim$100 TeV) at SNR shocks, cementing the long-suspected link between SNRs and cosmic rays. In addition, recent detections of TeV and GeV gamma-rays from some SNRs have also suggested acceleration of protons which are the majority of cosmic rays (McEnery *et al.* 2017).

RX J1713.7-3946, the X-ray image of which is presented in Fig. 1 left, is the brightest X-ray synchrotron and TeV gamma-ray SNR in our Galaxy, making it an exceptionally important object for the study of cosmic-ray acceleration (Koyama *et al.* 1997; Aharonian *et al.* 2007). Despite its importance, there are many unresolved problems with this SNR. For example, we do not know if the gamma-ray emission is dominated by accelerated protons (e.g., Uchiyama *et al.* 2007; Fukui *et al.* 2012; Sano *et al.* 2013) or electrons (e.g., Abdo *et al.* 2011; Lee *et al.* 2012). One of the key parameters to reveal their relative contributions is the ambient density. In most SNRs, ambient densities can be estimated by the analysis of thermal X-ray emission, whereas RX J1713.7-3946 does not allow for such estimates, because its X-ray emission is dominated by synchrotron radiation; despite extensive studies for two decades since its discovery, no thermal line emission had been detected (e.g., Tanaka *et al.* 2008). Recently, Katsuda *et al.* (2015) reported the first detection of thermal X-rays from the central region of the remnant. The thermal X-ray emission is likely to originate from shocked SN ejecta, rather than the shocked interstellar

https://doi.org/10.1017/S1743921317004434 Published online by Cambridge University Press

medium (ISM). Without information on the ISM, expansion measurements of the X-ray remnant would be the best hope for constraining the ambient densities. Tsuji & Uchiyama (2016) and Acero *et al.* (2017) recently succeeded in measuring proper motions in the northwestern and the southeastern filaments, respectively. Here, we concisely review the results of Katsuda *et al.* (2015) and Acero *et al.* (2017), including new information on the analysis and discussions.

2. Observations

We utilized archival XMM-Newton data for our spectral analysis that focuses on the central region of the remnant. The data include Obs.IDs 0207300201 (MOS1+MOS2), 0722190101 (MOS2), and 0740830201 (MOS1+MOS2), resulting in an effective exposure time of 375 ks for one MOS sensor. To measure proper motions in the southeastern rim, we used two data sets (Obs.IDs 0093670401 and 0743030101) with a time baseline of 13 yr. The first- and second-epoch data were taken on March 14, 2002 and March 11, 2015 with the effective exposure times of 11.7/5.7 ks (MOS/pn) and 64.1/48.0 (MOS/pn), respectively.

3. Spectral Analysis

We first generated a softness-ratio map from the XMM-Newton data, to identify best locations where thermal X-ray emission might be detectable. The idea is that softer regions should be promising sites for searching for thermal X-ray emission, because both less absorption and fainter synchrotron emission make the spectrum softer, enhancing the presence of thermal X-rays in the dominant synchrotron continuum. While Katsuda *et al.* (2015) selected the relatively small, softest area around the center of the remnant, we here enlarge the area by including its northern vicinity, so that we can improve the photon statistics. The updated region is shown as an ellipse in Fig. 1 left.

Figure 1 right exhibits the non X-ray background-subtracted XMM-Newton (MOS1+2) spectrum, from which we confirm that the line features at 1 keV (Ne Lyα), 1.35 keV (Mg Heα), and 1.85 keV (Si Heα) are clearly detected. We fit it by an absorbed thermal plus power-law component model with additional components for the sky background (OFF1 in Katsuda *et al.* (2015)). The best-fit model is shown in Fig. 1 right, and the best-fit parameters are listed in Table 1. We estimated the abundance ratios of Mg/Ne, Si/Ne, and Fe/Ne to be $\sim$2.3, $\sim$2.0, and $\sim$0.16, respectively. The Mg/Ne and Si/Ne ratios are consistent with those in Katsuda *et al.* (2015), whereas the Fe/Ne ratio is slightly higher than the previous work, which is probably due to the imperfect modeling of the sky background. That Fe is deficit in this plasma strongly suggests that it originates from core-collapse SN ejecta.

Table 1. Best-fit parameters

$N_{\rm H}$ (10^{21} cm^{-2})	Γ	$kT_{\rm e}$ (keV)	$\log(n_{\rm e}t)$ (cm^{-3} s)	Ne	Mg	Si	Fe	χ^2/d.o.f.
6.0$\pm$0.1	$2.29^{+0.02}_{-0.1}$	$0.58^{+0.22}_{-0.09}$	11.7$\pm$0.1	$3.1^{+4.8}_{-0.4}$	$7.1^{+10.9}_{-0.7}$	$6.1^{+9.1}_{-1.7}$	$0.5^{+0.7}_{-0.1}$	492 / 339

Notes:
The values of elemental abundances are multiples of solar values. Other elemental abundances are fixed to the solar values according to Wilms *et al.* (2001).

https://doi.org/10.1017/S1743921317004434 Published online by Cambridge University Press

4. Proper-Motion Measurements

To guide our region definition, we ran a Canny edge detection algorithm, because the exact shape and edge position of the SNR are not easy to determine by eye. The resulting edges, shown as contours in the upper panel of Fig. 2, perfectly outline the shape of the SNR edges, even in faint regions where the filament fades out. Based on the edge images shown in Fig. 2, two main structures labeled "outer region" and "inner region" (towards the inside of the SNR which is probably due to projection effects) were identified as promising regions to investigate the filament's proper motion. We used four X-ray point sources for our image alignment by using the SAS tool `eposcorr`. After alignment, the mean 2002-2015 residual offset of the four registration sources is 0.9 arcsec, which we consider as our systematical uncertainty.

To estimate the proper motion between the two epochs, we built a shock profile model based on the 2015 high statistic observation (assuming no errors), which is then compared to the 2002 profile (see Fig. 2 lower panels). The latter profile is in counts and is the sum of the MOS1 and MOS2 camera. We note that the number of counts for some bins of the 2002 radial profile falls below 25 counts per bins and we have therefore used Cash statistics (Cash 1979) rather than the χ^2 estimator. We calculate the C-value for various shifts and amplitudes (the intensity ratio between the 2002 and 2015 profiles), finding the best-fit shifts to be $0.61\pm0.05(\mathrm{stat.})\pm0.07(\mathrm{sys.})''\,\mathrm{yr}^{-1}$ and $0.75^{+0.05}_{-0.06}(\mathrm{stat.})\pm0.07(\mathrm{sys.})''\,\mathrm{yr}^{-1}$ for the inner and outer regions, respectively. These can be translate into shock speeds of $2880\pm240(\mathrm{stat.})\pm330(\mathrm{sys.})\,\mathrm{km\,s}^{-1}$ and $3550^{+250}_{-290}(\mathrm{stat.})\pm330(\mathrm{sys.})\,\mathrm{km\,s}^{-1}$ at a distance of 1 kpc (Fukui *et al.* 2003).

5. Discussion & Conclusions

We have detected X-ray line emission from the synchrotron-dominated SNR RX J1713.7-3946, thanks to the long integrated XMM-Newton exposure. We measured the abundance ratios of Mg/Ne, Si/Ne, and Fe/Ne in the thermal component to be ∼2.3, ∼2.0, and ∼0.16, respectively. The deficit of the Fe abundance immediately tells us that this emission originates from core-collapse SN ejecta rather than the swept-up ISM. The abundance pattern among Ne, Mg, and Si is consistent with those expected for relatively low-mass, $\lesssim$20 $\mathrm{M}_\odot$, progenitor stars rather than higher-mass progenitors (e.g., Tominaga *et al.* 2007).

Single stars whose masses are $\lesssim$20 $\mathrm{M}_\odot$ should result in SNe IIP from a theoretical point of view (Heger *et al.* 2003). Also, Wang *et al.* (1997) estimated the absolute magnitude at maximum light was probably between -12 and -14, implying a highly subluminous core-collapse SN event. For low-luminosity Type IIP events, the initial shock speeds are known to range from $\sim$2000 $\mathrm{km\,s}^{-1}$ to $\sim$6000 $\mathrm{km\,s}^{-1}$ (Spiro *et al.* 2014). This conflicts with the case for RX J1713.7-3946, for which the initial blastwave must be faster than $\sim$6000 $\mathrm{km\,s}^{-1}$, i.e., the current SNR radius of 9.6 pc divided by the age of 1600 yr inferred from the potential association with SN 393 (Wang *et al.* 1997). Instead, the relatively fast blastwave speed suggests that the SN of RX J1713.7-3946 was a stripped envelope, Type Ib/c or Type IIb, event. The apparent discrepancy between the abundance pattern and the shock speed could be explained if RX J1713.7-3946 arose from a Type Ib/c (or IIb) explosion of a relatively low-mass star forming a close binary, in which the (low-mass) progenitor had experienced a binary interaction to remove its massive H envelope.

In order to estimate the age and the ambient density, we compared proper motions measured in the southeastern rim with an SNR evolutionary model in Tang & Chevalier (2017), obtaining an age of $2250\pm170(\mathrm{stat.})\pm200(\mathrm{sys.})$ yr or $1760\pm130(\mathrm{stat.})\pm150(\mathrm{sys.})$

https://doi.org/10.1017/S1743921317004434 Published online by Cambridge University Press

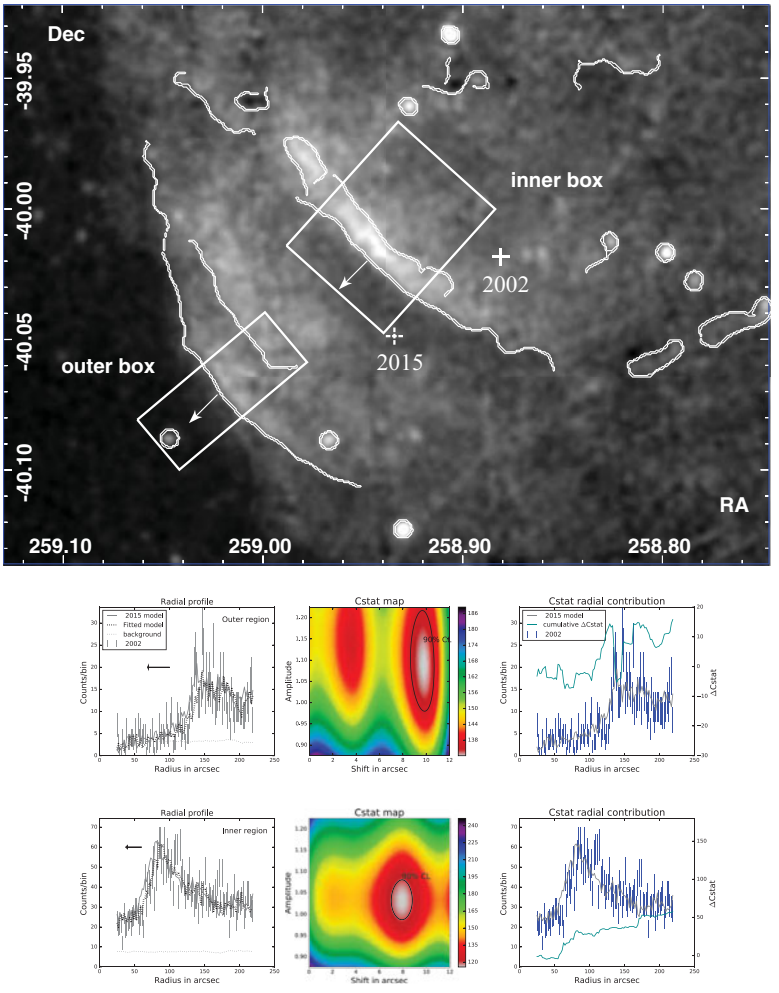

Figure 2. Upper panel: Exposure corrected and background subtracted count map in the 0.6–6 keV energy band of the 2015 XMM-Newton observation. The white contours are the results of the Canny edge detection algorithm. The white boxes represent the regions used to extract the radial profiles shown in lower panels, and the white crosses are the 2002 and 2015 pointing positions. The arrows indicate the direction of the shock motion. The middle-row panels: Radial profiles, C-stat maps and C-stat radial contribution from the outer region defined in the upper panel. The arrow in the left panel indicates the direction of the shock motion. We fit the 2002 profiles by 2015-based models with free normalizations and shifts, obtaining the best-fit models named "Fitted model". The right panel shows the cumulative statistics radial contribution (C-stat $= C_0(r) - C_{\rm bestfit}(r)$) taken at the best-fitted amplitude and where $C_0(r)$ is the Cstat radial contribution at a 0 arcsec model shift. The bottom-row panels: Same as the middle-row panels, but for the inner region defined in the upper panel.

yr in the case where the shock is evolving in a wind profile ($\rho \propto r^{-s}, s = 2$) or in a uniform medium ($s = 0$), respectively. In both cases, we derived an upstream density of the order of 0.01 cm^{-3}, compatible with the lack of thermal X-rays from the shocked ISM. The ages roughly agree with that of SN 393.

We perform another age estimate, based on a simple comparison of expansion indices (m) measured for several SNRs; $m = d(\log R)/d(\log t) = (dR/dt)/(R/t) = \mu/R\ t$, where R is the angular radius of the filament whose proper motion (μ) has been measured and

https://doi.org/10.1017/S1743921317004434 Published online by Cambridge University Press

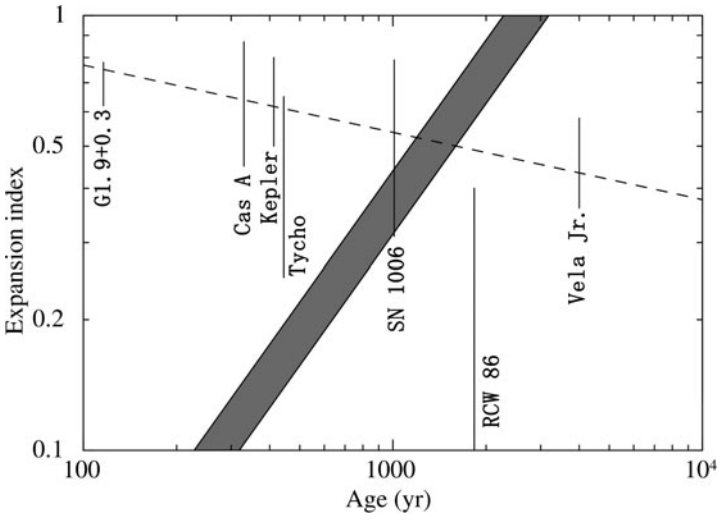

Figure 3. Expansion indices against the ages of young Galactic SNRs together with the best-fit power-law model shown as a dashed line. The red area indicates the 90% confidence interval for the m-value of RX J1713.7-3946.

t is the age of the remnant. Figure 3 plots m-values for several SNRs (Katsuda *et al.* 2016). The best-fit power-law function is shown as a dashed line. The red area indicates the 90% confidence interval for the m-value of RX J1713.7-3946, calculated from the proper motion of 0.62–$0.87''\,\mathrm{yr}^{-1}$ and the SNR radius of $33'$. This allows us to estimate an age of ∼1200–1600 yr, consistent with the idea that RX J1713.7-3946 is the remnant of SN 393.

This work is supported by the Japan Society for the Promotion of Science KAKENHI grant number 16K17673 (SK).

References

Abdo, A. A., *et al.* (Fermi Collaboration) 2011, *ApJ*, 734, 28
Acero, F., Katsuda, S., Ballet, J., & Petre, R. 2017, *A& A*, 597, 106
Aharonian, F. A., *et al.* (HESS Collaboration) 2017, *A& A*, 464, 235
Cash, W. 1979, *ApJ*, 228, 939
Fukui, Y., Moriguchi, Y., Tamura, K., *et al.* 2003, *PASJ*, 55, L61
Fukui, Y., Sano, H., Sato, J., *et al.* 2012, *ApJ*, 746, 82
Heger, A., Fryer, C. L., Woosley, S. E., Langer, N., & Hartmann, D. H. 2003, *ApJ*, 591, 288
Katsuda, S., Acero, F., & Tominaga, N., *et al.* 2015, *ApJ*, 814, 29
Katsuda, S., Tanaka, M., Morokuma, T., Fesen, R., & Milisavljevic, D. 2016, *ApJ*, 826, 108
Koyama, K., Petre, R., Gotthelf, E. V., Hwang, U., Matsuura, M., Ozaki, M., & Holt, S. S. 1995, *Nature*, 378, 255
Koyama, K., Kinugasa, K., Matsuzaki, K., Nishiuchi, M., Sugizaki, M., Torii, K., Yamauchi, S., & Aschenbach, B. 1997, *PASJ*, 49, L7
Lee, S.-H., Ellison, D., & Nagataki, S. 2012, *ApJ*, 750, 156
McEnery, J. *et al.* 2017, *these poceedings*
Sano, H., Tanaka, T., Torii, K., *et al.* 2013, *ApJ*, 778, 59
Spiro, S., Pastorello, A., Pumo, M. L., *et al.* 2014, *MNRAS*, 439, 2873
Tominaga, N., Umeda, H., & Nomoto, K. 2007, *ApJ*, 660, 516
Tang, X. & Chevalier, R. A. 2017, *MNRAS*, 465, 3793
Tanaka, T., Uchiyama, Y., Aharonian, F. A., *et al.* 2007, *ApJ*, 685, 988

Tsuji, N. & Uchiyama, Y. 2016, *PASJ*, 68, 108
Uchiyama, Y., Aharonian, F. A., Tanaka, T., Takahashi, T., & Maeda, Y. 2007, *Nature*, 449, 576
Wang, Z. R., Qu, Q.-Y., & Chen, Y. 1997, *A& A*, 318, L59
Wilms, J., Allen, A., & McCray, R. 2000, *ApJ*, 542, 914

https://doi.org/10.1017/S1743921317004434 Published online by Cambridge University Press